Received: 2 January 2022 | Revised: 25 January 2022 | Accepted: 30 January 2022

DOI: 10.1002/jbio.202200001

RESEARCH ARTICLE

JOURNAL OF BIOPHOTONICS

Surface plasmon resonance biosensor based on graphene layer for the detection of waterborne bacteria

Malek G. Daher[1] | **Sofyan A. Taya**[1,2*] | **Ilhami Colak**[3] | **Shobhit K. Patel**[4] | **Melad M. Olaimat**[2] | **Omar Ramahi**[2]

[1]Department of Physics, Islamic University of Gaza, Gaza, Palestine

[2]Department of Electrical and Computer Engineering, University of Waterloo, Waterloo, Ontario, Canada

[3]Department of Electrical and Electronics Engineering, Nisantasi University, Istanbul, Turkey

[4]Department of Computer Engineering, Marwadi University, Rajkot, India

***Correspondence**
Sofyan A. Taya, Department of Electrical and Computer Engineering, University of Waterloo, Waterloo, Ontario N2L 3G1, Canada.
Email: staya@iugaza.edu.ps

Funding information
Arab Fund for Economic and Social Development

Abstract

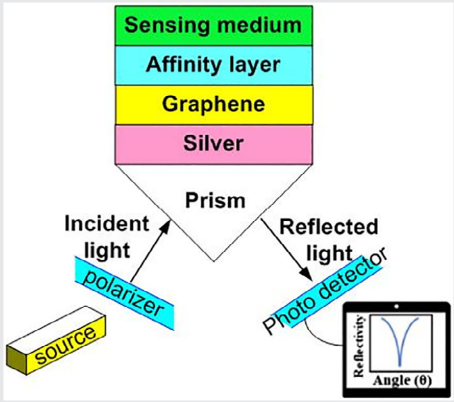

As a result of the risks that waterborne bacteria bring to the human body, identifying them in drinking water has become a global concern. In this article, a highly sensitive surface plasmon resonance (SPR) biosensor consisting of prism, Ag, graphene, affinity layer and sensing medium is proposed for rapid detection of the waterborne bacteria. Four SPR-based sensors are first studied with the structures prism/Ag/sensing medium, prism/Ag/affinity layer/sensing medium, prism/Ag/graphene/sensing medium, and prism/Ag/graphene/affinity layer/sensing medium. The latter structure is found to have the highest sensitivity so it is considered for further investigations. Four different commonly used prisms are then demonstrated which are N-FK51A, 2S2G, SF10 and BK7. The structure with the prism N-FK51A is found to correspond to the highest sensitivity so it is considered for further investigations. The structure parameters are then optimized. The proposed SPR sensor can achieve high sensitivity of about 221.63 °/RIU for *Escherichia coli* and 178.12 °/RIU for *Vibrio cholera* bacteria with an average value of 199.87 °/RIU. We believe that the proposed structure will open a new window in the field of microorganism detections.

KEYWORDS

graphene, sensitivity, sensor, surface plasmon resonance, waterborne bacteria

1 | INTRODUCTION

Drinking water that is infected with bacteria, viruses or parasites can cause a variety of diseases, including waterborne infections. *Escherichia coli* (*E. coli*) and *Vibrio cholera* (*V. cholera*) are two examples of waterborne bacteria that can cause waterborne infections. A waterborne illness occurs when feces from animals or humans get into the drinking water. Infected animals can include poultry, livestock, pets or wild animals like rodents, deer and beaver. Septic fields, sewer pipes, runoff from landfills, residential/human waste or industrial developments can also contaminate surface water that is used as drinking water. Public and private drinking water systems are more likely to suffer from contamination if they receive their drinking water from surface water sources such as lakes or streams. As a result, developing a real-time and sensitive detector for waterborne bacteria identification is vital.

Surface plasmon resonance (SPR), a subset of surface plasmons (SPs), exhibits a wide range of unique optical features, including varying resonant frequencies in host media with varying refractive indices. Many practical applications in biosensors to detect and characterize chemical and biological substances have been discovered due to SPR's unique optical features [1–6]. SPR-based sensors show many advantages such as high reliability and real-time analysis with high sensitivity [7]. The operating principle of SPR sensors is based on detecting shifts in resonance in the optical spectrum caused by changes in the refractive index of the sensing medium [8] when molecules are deposited on the detecting element's surface. The Kretschmann arrangement is extensively used to excite SPs in traditional SPR sensors [9], and a thin metal layer is generally deposited on the top of a prism to adsorb chemical or biological molecules. However, due to metals' low adsorbability, researchers are looking for alternative materials to increase biosensor performance. Graphene emerges as one of the possible solutions. It is a two-dimensional plane of sp2 connected carbon atoms made out of a single sheet of graphite. The atoms are organized in a one-atom-thick honeycomb lattice structure [10]. It has received a lot of attention because of its amazing optical and electrical qualities, its higher surface to volume ratio and stronger π stacking interaction between its hexagonal cells and the carbon-based ring structures. It exhibits exceptionally effective biomolecule adsorption [11]. As a result, graphene is frequently regarded as an alternate material for improving biosensor adsorbability. SPR sensor sensitivity plays a significant role to detect resonance changes. To enhance the performance of such sensors, an extra layer is added between the graphene and metal layers [12], such as MoS_2 sheets, black phosphorus, silicon and metamaterial. The low sensitivity problem and large full width at half maximum are still suspended in SPR structures. An extra layer of $BaTiO_3$, which shows exceptional dielectric characteristics, such as high refractive index and low loss, has been demonstrated to give a significant shift in resonance angle within a modest change in the refractive index [13–15].

The detection of circulating miRNA as a breast cancer biomarker in patient sera was reported. An imaging biosensor based on surface plasmon resonance was employed [16]. An optical stimulation strategy to create intracellular Ca^{2+} transients of astrocytes was shown by employing near-infrared light and localized surface plasmon resonance [17].

In this article, an SPR biosensor consisting of prism, Ag, graphene, affinity layer and sensing medium is proposed for waterborne bacteria detection. The reflection intensity is studied by employing the transfer matrix method. Four structures are first studied. The structure with the highest sensitivity is then considered for further investigations. Four different prisms are then demonstrated. The prism that corresponds to the highest sensitivity is then considered for further investigations. The parameters of the SPR biosensor are then optimized.

2 | DESIGN AND THEORETICAL MODEL

2.1 | Model design

An SPR-based biosensor is proposed for the detection of waterborne bacteria. The proposed structure comprises five layers: prism, Ag, graphene, affinity layer and sensing medium. The thicknesses of silver, graphene and affinity layers are d_{Ag}, d_g and d_{Aff} and the refractive indices are n_{Ag}, n_g and n_{Aff}, respectively. Figure 1 shows a schematic diagram of the proposed SPR biosensor based on a graphene layer.

There are many types of prisms that can affect the SPR biosensor performance. The most commonly used are N-FK51A, 2S2G, SF10 and BK7 glass prisms. The refractive index of SF10 glass prism is $n_p = 1.723$ [18]. The refractive index of the N-FK51A glass prism depends on the radiation wavelength according to the following relation [19]:

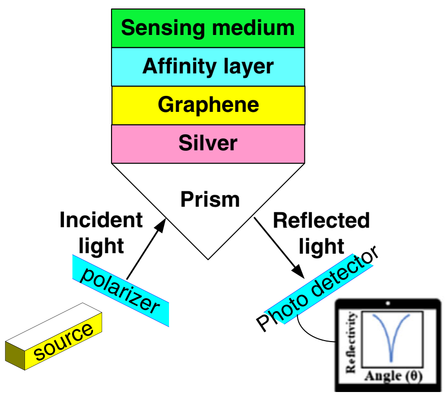

FIGURE 1 Schematic diagram of an SPR biosensor based on a graphene layer

$$n(\lambda)=\sqrt{1+\frac{a_1\lambda^2}{\lambda^2-b_1}+\frac{a_2\lambda^2}{\lambda^2-b_2}+\frac{a_3\lambda^2}{\lambda^2-b_3}} \quad (1)$$

where a_1, a_2, a_3, b_1, b_1 and b_3 are the Sellmeier coefficients which are given as $a_1 = 0.971247817$, $a_2 = 0.216901417$, $a_3 = 0.904651666$, $b_1 = 0.00472301995$, $b_2 = 0.0153575612$ and $b_3 = 168.68133$. λ is the wavelength of incident light in µm. The refractive index of the chalcogenide prism (2S2G) is given by the following relation [20]:

$$n(\lambda)=c_1+\frac{c_2}{\lambda^2}+\frac{c_3}{\lambda^4} \quad (2)$$

where $c_1 = 2.24047$, $c_2 = 2.693\times10^{-2}$ and $c_3 = 8.08\times10^{-3}$.

The index of refraction of BK7 glass prism can be calculated according to the following equation [21]:

$$n(\lambda)=\sqrt{1+\frac{d_1\lambda^2}{\lambda^2-e_1}+\frac{d_2\lambda^2}{\lambda^2-e_2}+\frac{d_3\lambda^2}{\lambda^2-e_3}} \quad (3)$$

where $d_1 = 1.03961212$, $d_2 = 1.01046945$, $d_3 = 0.231792344$, $e_1 = 0.00600069867$, $e_2 = 103.560653$ and $e_3 = 0.0200179144$.

The incident light wavelength-dependent refractive index of the Ag layer is given by the Drude-Lorentz model [22]:

$$n(\lambda)=1-\frac{\lambda_c\lambda^2}{\lambda_p{}^2(\lambda_c+i\lambda)} \quad (4)$$

where $\lambda_c=1.7614\times10^{-5}$ m and $\lambda_p=1.4541\times10^{-7}$ m are the collision and plasma wavelengths of Ag. i is the complex number.

The refractive index of graphene can be calculated using the following equation [23]:

$$n(\lambda)=3+\lambda\frac{C}{3}i \quad (5)$$

where C is a constant equal to 5.446 µm^{-1}. Finally, we have considered an affinity layer with a refractive index of 1.5265 (nicotine).

2.2 | Mathematical modeling

All layers are arranged in a stack along the z-axis. For each layer, the dielectric constant and the thickness are ε_k and d_k, respectively. The tangential field at the first boundary ($z = 0$) and that at the final boundary ($z = z_{N-1}$) are related to each other through [24]:

$$\begin{bmatrix}F_1\\G_1\end{bmatrix}=P\begin{bmatrix}F_{N-1}\\G_{N-1}\end{bmatrix} \quad (6)$$

where F_1 and F_{N-1} are the tangential electric fields at the first and Nth interfaces, respectively, and G_1 and G_{N-1} are the tangential magnetic fields at the first and Nth interfaces, respectively. For the jth layer, the characteristic matrix (P_j) is given by:

$$P_j=\begin{bmatrix}\cos(\alpha_j) & -\frac{i\sin(\alpha_j)}{Y_j}\\ -iY_j\sin(\alpha_j) & \cos(\alpha_j)\end{bmatrix} \quad (7)$$

α_j is the phase variation of the light wave propagating through the jth layer which is given by [24]:

$$\alpha_j=\frac{2\pi}{\lambda}d_j\left(\varepsilon_j-(n_1\sin\theta_1)^2\right)^{0.5} \quad (8)$$

where ε_j and d_j are the dielectric permittivity and thickness of the jth layer. λ, θ_1 and n_1 are the incident light wavelength, the angle of incidence and the prism refractive index.

We restrict the study to TM polarization since the SPR waves cannot be excited in another mode unless we have a material of simultaneously negative permittivity and permeability. For transverse magnetic (TM) waves $Y_j=\left(\varepsilon_j-(n_1\sin\theta_1)^2\right)^{0.5}/\varepsilon_j$. The total transfer matrix P of the structure can be expressed as:

$$P=P_{\mathrm{Ag}}P_{\mathrm{g}}P_{\mathrm{Aff}}=\begin{bmatrix}P_{11} & P_{12}\\ P_{21} & P_{22}\end{bmatrix} \quad (9)$$

where P_{Ag}, P_{g} and P_{Aff} are the transfer matrices of the silver, graphene and affinity layers, respectively.

The reflection coefficient (r) through the structure for TM waves (p-polarized) can be expressed as

$$r=\frac{(P_{11}+P_{12}Y_N)Y_1-(P_{21}+P_{22}Y_N)}{(P_{11}+P_{12}Y_N)Y_1+(P_{21}+P_{22}Y_N)} \quad (10)$$

Finally, the reflection intensity (R) for hybrid N-layer structure can be given by:

$$R=|r|^2 \quad (11)$$

The sensitivity of an SPR sensor is calculated as:

$$S = \Delta\theta_{res}/\Delta n, \quad (12)$$

where $\Delta\theta_{res}$ and Δn are the difference in the resonant angle and the refractive index, respectively. This difference is calculated between an analyte and a reference sample.

3 | RESULTS AND DISCUSSION

3.1 | Waterborne bacteria sensor

Different structures are first investigated to show the priority of the proposed structure at a wavelength of 632.8 nm. The refractive indices of the layers are calculated at a wavelength of 632.8 nm according to the equations given in section 2. They are found as $n_p = 1.723$, $n_{Ag} = 0.056206 + 4.2776\,i$, $n_g = 3 + 1.149106\,i$ and $n_{Aff} = 1.5265$ for SF10 glass prism, silver, graphene and Affinity layer. The thicknesses of these layers are taken as $d_{Ag} = 45\,\text{nm}$, $d_g = M \times 0.34\,\text{nm}$ where M is the number of graphene sheets ($M = 1$) and $d_{Aff} = 3\,\text{nm}$. It is worth mentioning that pure water is used as reference material.

The first structure is chosen as SF10 glass prism/Ag/sensing medium such that the sensing medium is taken as a waterborne sample. The resonant angles are found at 54.64°, 56.83° and 58.50° for the samples of pure water, *V. cholera* and *E. coli*. The refractive indices of *V. cholera* and *E. coli* can be found in reference [24]. The sensitivities are calculated and found as 68.43 and 70.18 °/RIU for the samples of *V. cholera* and *E. coli*, respectively. The results of the structure SF10 glass prism/Ag/sensing medium are presented in Table 1. The second structure is taken as SF10 glass prism/Ag/affinity layer/sensing medium and the resonant angles are found at 54.93°, 57.13° and 58.80° for the samples of pure water, *V. cholera* and *E. coli*. The sensitivities are calculated and found as 68.75 and 70.36 °/RIU for the samples of *V. cholera* and *E. coli*, respectively as presented in Table 2. The third structure is taken as SF10 glass prism/Ag/graphene/sensing medium. The resonant angles of the current structure are found at 54.78°, 57° and 58.70° for the three samples. The sensitivities are calculated and found as 69.37 and 71.27 °/RIU for the samples of *V. cholera* and *E. coli*, respectively. The results of this structure are given in Table 3. The fourth structure is taken as SF10 glass prism/Ag/graphene/affinity layer/sensing medium and the resonant angles are found at 55.08°, 57.31° and 59.01°. The sensitivities are calculated and found as 69.68 and 71.45 °/RIU for the samples of *V. cholera* and *E. coli*, respectively, as shown in Table 4. Figure 2 shows the reflected intensity of the proposed SPR sensor for the structures SF10 glass prism/Ag/sensing medium (Figure 2A), SF10 glass prism/Ag/affinity layer/sensing medium (Figure 2B), SF10 glass prism/Ag/graphene/sensing medium (Figure 2C) and SF10 glass prism/Ag/graphene/affinity layer/sensing medium (Figure 2D). As can be seen from Tables 1–4, there is no significant difference between the four structures. The fourth SPR-based sensor with the structure SF10 glass prism/Ag/graphene/affinity layer/sensing medium shows a little bit improved sensitivity over other structures so it will be adopted for the next investigations.

3.2 | Selection of the prism type

In this subsection, four different prisms are investigated. The first prism is taken as N-FK51A glass whose refractive index of 1.4853 at a wavelength of 632.8 nm so that the current structure has the form N-FK51A glass prism/Ag/graphene/affinity layer/sensing medium. The resonant angles are found at 71.71°, 76.78° and 81.87° for the samples of the pure water, *V. cholera* and *E. coli*. The sensitivities are calculated as 158.43°and 184.72 °/RIU for the samples of *V. cholera* and *E. coli*, respectively, as shown in Table 5. The second prism is taken as BK7 glass with a refractive index of 1.5151 at a wavelength of 632.8 nm. The structure we have now becomes BK7 glass prism/Ag/graphene/affinity layer/sensing medium and the resonant angles are found at 68.64°, 72.74° and 76.39° for the three samples. The sensitivities are calculated and found as 128.12 and 140.90 °/RIU for *V. cholera* and *E. coli*, respectively, as shown in Table 6. The third prism is chosen as SF10 glass with a refractive index of 1.723 at a wavelength of 632.8 nm. The resonant angles are found

TABLE 1 Resonant dip position and sensitivity of the SPR-based sensor consisting of SF10 glass prism/Ag/sensing medium ($\lambda = 632.8\,\text{nm}$, $d_{Ag} = 45\,\text{nm}$, $d_g = M \times 0.34\,\text{nm}$, $M = 1$, $d_{Aff} = 3\,\text{nm}$)

Waterborne bacteria	Refractive index	Position of resonant dip (°)	Resonant angle shift (°)	Sensitivity (°/RIU)
Pure water	1.333	54.64	–	–
V. cholera	1.365	56.83	2.19	68.43
E. coli	1.388	58.50	3.86	70.18

TABLE 2 Resonant dip position and sensitivity of the SPR-based sensor consisting of SF10 glass prism/Ag/affinity layer/sensing medium ($\lambda = 632.8$ nm, $d_{Ag} = 45$ nm, $d_g = M \times 0.34$ nm, $M = 1$, $d_{Aff} = 3$ nm)

Waterborne bacteria	Refractive index	Position of resonant dip (°)	Resonant angle shift (°)	Sensitivity (°/RIU)
Pure water	1.333	54.93	–	–
V. cholera	1.365	57.13	2.2	68.75
E. coli	1.388	58.80	3.87	70.36

TABLE 3 Resonant dip position and sensitivity of the SPR-based sensor consisting of SF10 glass prism/Ag/graphene/sensing medium ($\lambda = 632.8$ nm, $d_{Ag} = 45$ nm, $d_g = M \times 0.34$ nm, $M = 1$, $d_{Aff} = 3$ nm)

Waterborne bacteria	Refractive index	Position of resonant dip (°)	Resonant angle shift (°)	Sensitivity (°/RIU)
Pure water	1.333	54.78	–	–
V. cholera	1.365	57	2.22	69.37
E. coli	1.388	58.70	3.92	71.27

TABLE 4 Resonant dip position and sensitivity of the SPR-based sensor consisting of SF10 glass prism/Ag/graphene/affinity layer/sensing medium ($\lambda = 632.8$ nm, $d_{Ag} = 45$ nm, $d_g = M \times 0.34$ nm, $M = 1$, $d_{Aff} = 3$ nm)

Waterborne bacteria	Refractive index	Position of resonant dip (°)	Resonant angle shift (°)	Sensitivity (°/RIU)
Pure water	1.333	55.08	–	–
V. cholera	1.365	57.31	2.23	69.68
E. coli	1.388	59.01	3.93	71.45

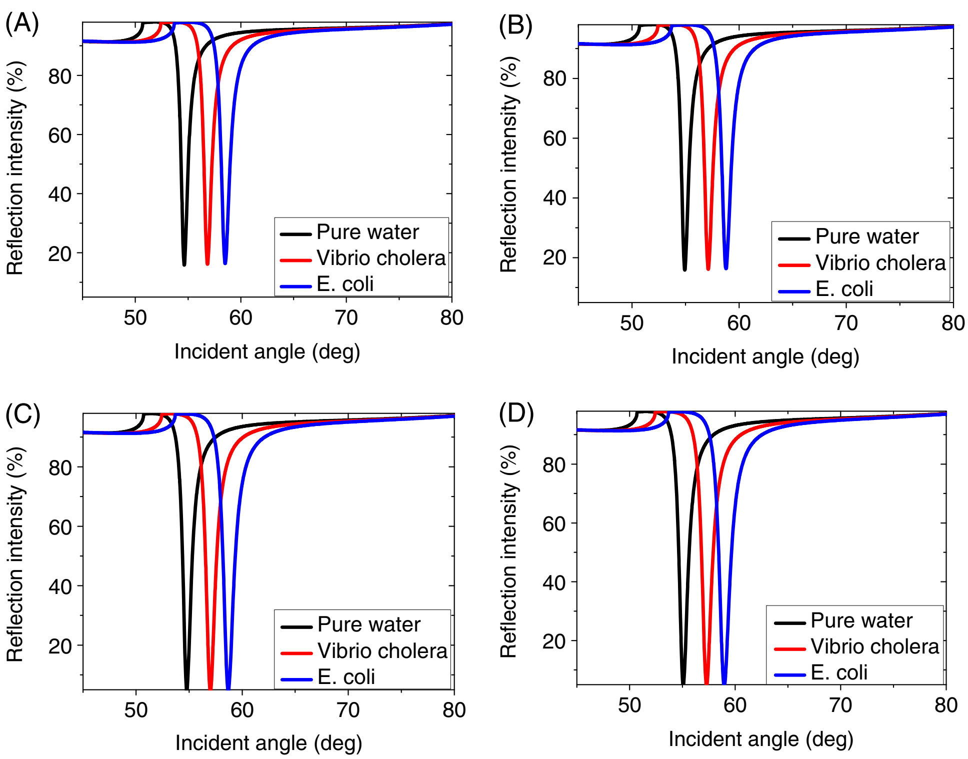

FIGURE 2 Reflectance curves of the proposed SPR sensor with different structures (A) SF10 glass prism/Ag/sensing medium, (B) SF10 glass prism/Ag/affinity layer/sensing medium, (C) SF10 glass prism/Ag/graphene/sensing medium and (D) SF10 glass prism/Ag/graphene/affinity layer/sensing medium

at 55.08°, 57.31° and 59.01° for the samples of pure water, *V. cholera* and *E. coli*. The sensitivities are calculated and found as 69.68 and 71.45 °/RIU for the samples of *V. cholera* and *E. coli*, respectively, as shown in Table 7. Finally, the fourth prism is chosen as 2S2G glass with a refractive index of 2.358 at the same wavelength. The resonant angles are found at 36.81°, 37.95° and 38.79° for the samples of pure water, *V. cholera* and *E. coli*. The sensitivities are calculated and found as 35.62 and 36 °/RIU for the samples of *V. cholera* and *E. coli*, respectively, as shown in Table 8. Figure 3 shows the reflected intensity of the sensor for the prisms N-FK51A (Figure 3A), BK7 (Figure 3B), SF10 (Figure 3C) and 2S2G (Figure 3D). Resonant dip angles shift to a lower angle region when a higher refractive index prism is used and the sensitivity shows a shrink. In conclusion to this subsection, the sensitivity shows a significant improvement when the structure consists of a lower refractive index prism. The N-FK51A glass prism will be adopted in the next steps.

3.3 | Optimization of the structure parameters

The effects of some parameters such as metal layer thickness, number of graphene layers and affinity layer

TABLE 5 Resonant dip position and sensitivity of the SPR-based sensor consisting of N-FK51A glass prism/Ag/graphene/affinity layer/sensing medium at $n_p = 1.4853$

Waterborne bacteria	Refractive index	Position of resonant dip (°)	Resonant angle shift (°)	Sensitivity (°/RIU)
Pure water	1.333	71.71	–	–
V. cholera	1.365	76.78	5.07	158.43
E. coli	1.388	81.87	10.16	184.72

TABLE 6 Resonant dip position and sensitivity of the SPR-based sensor consisting of BK7 glass prism/Ag/graphene/affinity layer/sensing medium at $n_p = 1.5151$

Waterborne bacteria	Refractive index	Position of resonant dip (°)	Resonant angle shift (°)	Sensitivity (°/RIU)
Pure water	1.333	68.64	–	–
V. cholera	1.365	72.74	4.1	128.12
E. coli	1.388	76.39	7.75	140.90

TABLE 7 Resonant dip position and sensitivity of the SPR-based sensor consisting of SF10 glass prism/Ag/graphene/affinity layer/sensing medium at $n_p = 1.723$

Waterborne bacteria	Refractive index	Position of resonant dip (°)	Resonant angle shift (°)	Sensitivity (°/RIU)
Pure water	1.333	55.08	–	–
V. cholera	1.365	57.31	2.23	69.68
E. coli	1.388	59.01	3.93	71.45

TABLE 8 Resonant dip position and sensitivity of the SPR-based sensor consisting of 2S2G glass prism/Ag/graphene/affinity layer/sensing medium at $n_p = 2.358$

Waterborne bacteria	Refractive index	Position of resonant dip (°)	Resonant angle shift (°)	Sensitivity (°/RIU)
Pure water	1.333	36.81	–	–
V. cholera	1.365	37.95	1.14	35.62
E. coli	1.388	38.79	1.98	36

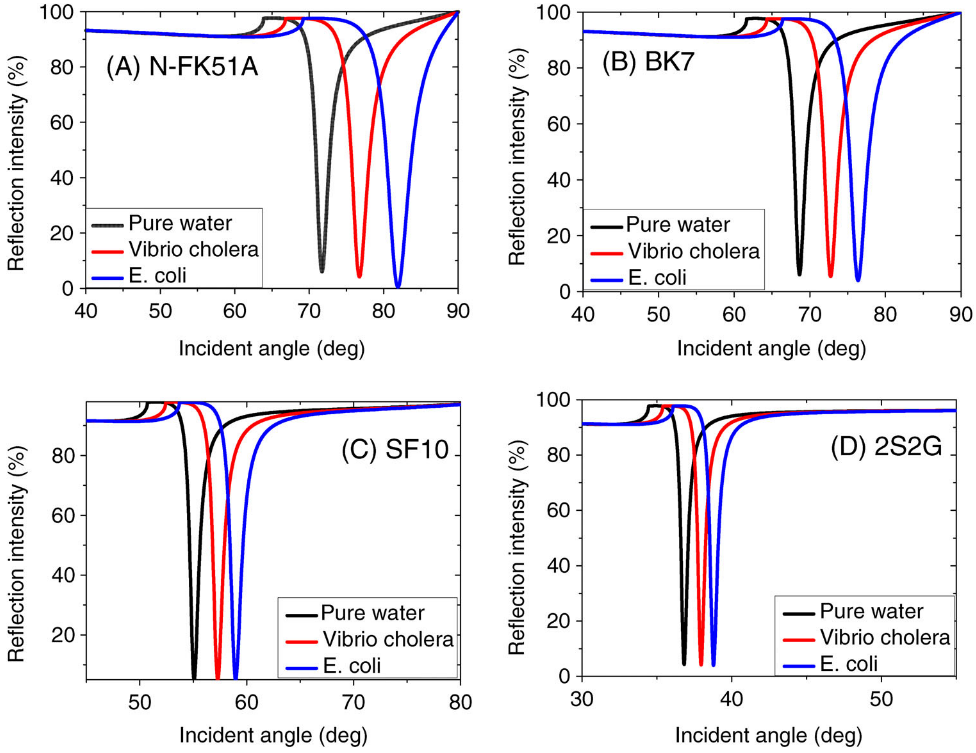

FIGURE 3 Reflectance curves of proposed the SPR sensor with the structure of prism/Ag/graphene/affinity layer/sensing medium for different types of the prism (A) N-FK51A, (B) BK7, (C) SF10 and (D) 2S2G ($\lambda = 632.8$ nm, $d_{Ag} = 45$ nm, $d_g = M \times 0.34$ nm, $M = 1$, $d_{Aff} = 3$ nm)

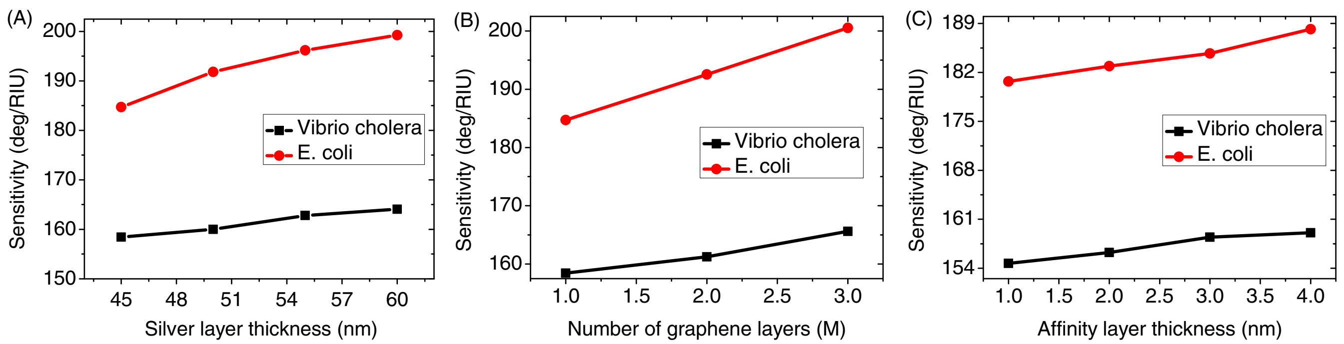

FIGURE 4 Optimization of the parameters of the structure N-FK51A glass prism/Ag/graphene/affinity layer/sensing medium. (A) Sensitivity versus the silver layer thickness. (B) Sensitivity versus the number of graphene layers. (C) Sensitivity versus the affinity layer thickness

thickness on the sensitivity of the SPR biosensor are investigated. The structure of N-FK51A glass prism/Ag/graphene/affinity layer/sensing medium is employed. Different thicknesses for the silver layer are used in the range 45 to 60 nm as shown in Figure 4A. The sensitivities to *V. cholera* are calculated and found as 158.43, 160, 162.81 and 164.06 °/RIU for a silver layer thickness of 45, 50, 55 and 60 nm, respectively. The sensitivities to *E. coli* are found as 184.72, 191.81, 196.18 and 199.27 °/RIU for a silver layer thickness of 45, 50, 55 and 60 nm, respectively. Therefore, the optimum thickness of the silver layer is 60 nm. For thickness <60 nm, the resonant dip is not observed in the reflectance curves.

The thickness of a graphene sheet is 0.34 nm. The graphene layer thickness is assumed $M \times 0.34$ nm, where M is the number of graphene sheets. The sensitivity to *V. cholera* (Figure 4B) is calculated and found as 158.43, 161.25 and 165.62 °/RIU for $M = 1$, 2 and 3, respectively. The sensitivity to *E. coli* is calculated and found as 184.72, 192.54 and 200.54 °/RIU for $M = 1$, 2 and 3, respectively. For $M > 3$, the resonant dip is not observed in the reflectance curves. Thus, the optimum number of graphene sheets is $M = 3$.

The affinity layer thickness is varied and the sensitivities are calculated for each case (Figure 4C). The sensitivity to *V. cholera* is found as 154.68, 156.25, 158.43 and

159.06 °/RIU for d_{Aff} = 1, 2, 3 and 4 nm, respectively whereas the sensitivity to *E. coli* is found as 180.72, 182.90, 184.72 and 188.18 °/RIU for d_{Aff} = 1, 2, 3 and 4 nm, respectively. For $d_{Aff} > 4$ nm, the resonant dip vanishes. So, the optimum affinity layer thickness is $d_{Aff} = 4$ nm.

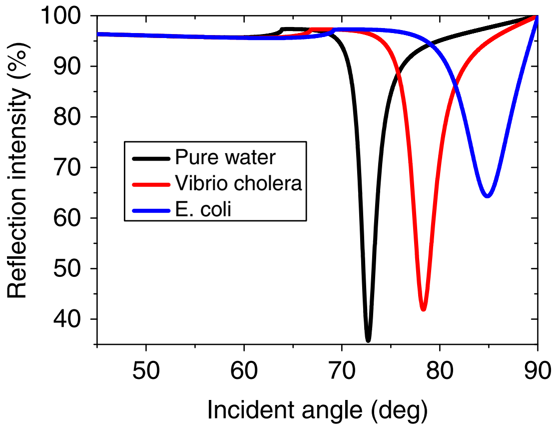

FIGURE 5 Reflectance curves of the proposed SPR sensor with the structure of N-FK51A glass prism/Ag/graphene/affinity layer/sensing medium at $\lambda = 632.8$ nm, $d_{Ag} = 60$ nm, $d_g = M \times 0.34$ nm, $M = 3$ and $d_{Aff} = 4$ nm

3.4 | The optimum waterborne bacteria sensor

Figure 5 shows the resonant dips of the SPR-based sensor for the samples of pure water, *V. cholera* and *E. coli*. The parameters are taken as the optimum conditions of $d_{Ag} = 60$ nm, $d_g = M \times 0.34$ nm, $M = 3$ and $d_{Aff} = 4$ nm. When the pure water is taken as a sensing medium, the resonant angle position is found at 72.67°. It is found that the resonant dip shifts to higher angles as the samples of waterborne bacteria are treated as sensing media. The new angles of the resonant dips are found at 78.37° and 84.86° nm for *V. cholera* and *E. coli*, respectively. The sensitivities are found as 178.12 and 221.63 °/RIU for the samples of *V. cholera* and *E. coli*, respectively as shown in Table 9. The average optimum sensitivity of the biosensor is 199.87 °/RIU, which, to the best of our knowledge, is a high value as compared with recently published articles. The quality factor and the detection accuracy of a dip are inversely proportional to the full width at half maximum. As can be seen, the dip of pure water is sharper than those of *V. cholera* and *E. coli* which means the quality factor and detection accuracy of pure water are higher than those of *V. cholera* and *E. coli*.

Table 10 presents a comparison of the proposed biosensor sensitivity with the most recent biosensing designs

TABLE 9 Resonant dip position and sensitivity of the SPR-based sensor consisting of N-FK51A glass prism/Ag/graphene/affinity layer/sensing medium ($d_{Ag} = 60$ nm, $d_g = M \times 0.34$ nm, $M = 3$, $d_{Aff} = 4$ nm)

Waterborne bacteria	Refractive index	Position of resonant dip (°)	Resonant angle shift (°)	Sensitivity (°/RIU)
Pure water	1.333	72.67	–	–
V. cholera	1.365	78.37	5.7	178.12
E. coli	1.388	84.86	12.19	221.63

Note: Average sensitivity = 199.87 °/RIU.

TABLE 10 Comparing the sensitivity of the current study with the most recent published biosensors based on SPR

Techniques/structures	Year	Sensitivity (°/RIU)	References
MoS_2-graphene hybrid-based fiber optic SPR biosensor	2017	105.71	[27]
Au-MoS_2-graphene based hybrid SPR biosensor	2017	89.29	[28]
Zinc oxide, gold and graphene-based SPR for the detection of pseudomonas like bacteria.	2018	187.43	[29]
SPR sensor modeling employing graphene tri sheets	2019	121.67	[30]
SPR biosensor using ZnO for DNA hybridization	2020	156.33	[25]
SPR optical sensor using a thin layer of plasma	2021	103	[26]
SPR biosensor based on graphene sheets for the detection of waterborne bacteria	2021	199.87	Current study

based on SPR. As an example, in 2020, an SPR biosensor using ZnO for DNA hybridization was proposed and the authors found a maximum sensitivity of 156.33 °/RIU [25]. In 2021, an SPR sensor using a thin layer of plasma was investigated and the attained sensitivity was found as 103 °/RIU [26]. The current proposed sensor achieved a high sensitivity of about 221.63 °/RIU for *E. coli* and 178.12 °/RIU for *V. cholera* with an average value of 199.87 °/RIU.

4 | CONCLUSION

An SPR biosensor has been proposed having the structure glass prism/Ag/graphene/affinity layer/sensing medium for the detection of waterborne bacteria. The reflected intensity has been deduced using the transfer matrix method. Four structures have been first investigated. These structures are prism/Ag/sensing medium, prism/Ag/affinity layer/sensing medium, prism/Ag/graphene/sensing medium and prism/Ag/graphene/affinity layer/sensing medium. There is no significant difference between the four structures. The latter one has been selected because it shows a little bit improved efficiency. Four different prisms have been examined which are N-FK51A, 2S2G, SF10 and BK7. The structure with the prism N-FK51A has been found to correspond to the highest sensitivity. By optimizing the thicknesses of Ag, affinity layer and the number of graphene layers, high sensitivity of 221.63 °/RIU for *E. coli* and 178.12 °/RIU for *V. cholera* has been obtained. We believe that the proposed structure will open a new window for promising versatile sensors.

ACKNOWLEDGMENT

The authors deeply acknowledge the financial support of the Arab Fund for Economic and Social Development.

CONFLICT OF INTEREST

The authors declare no conflict of interest.

DATA AVAILABILITY STATEMENT

The data that support the findings of this study are available on request from the corresponding author.

ORCID

Sofyan A. Taya https://orcid.org/0000-0001-5060-2534

REFERENCES

[1] Y. Singh, S. K. Raghuwanshi, *Optik* **2021**, *226*(1), 165842.
[2] K. Shah, N. K. Sharma, V. Sajal, *Opt Quant Electron* **2018**, *50*, 265.
[3] F. Haider, R. A. Aoni, R. Ahmed, A. E. Miroshnichenko, *J. Opt. Soc. Am. B* **2018**, *35*, 2816.
[4] L. Wei, C. Feng, L. Yuan, *Appl. Optics* **2020**, *59*, 2883.
[5] A. Dhibi, I. Sassi, M. Oumezzine, *Indian J Phys* **2016**, *90*, 125.
[6] S. Guo, X. Wu, Z. Li, et al., *Pramana: J Phys* **2021**, *95*, 66.
[7] E. J. Shin, W. G. Lee, S. J. Moon, *Microsyst Technol* **2016**, *22*, 2093.
[8] H. Yang, G. Wang, Y. Lu, et al., *Opt Quant Electron* **2021**, *53*, 341.
[9] L. Han, C. Xu, T. Huang, X. Dang, *Appl. Optics* **2021**, *60*, 1753.
[10] Y.-J. He, Y.-L. Lo, J.-F. Huang, *J. Opt. Soc. Am. B* **2006**, *23*, 801.
[11] J. Chen, B. Liu, *Eur. Phys. J. Plus* **2021**, *136*, 379.
[12] L. Liu, M. Wang, L. Jiao, T. Wu, F. Xia, M. Liu, W. Kong, L. Dong, M. Yun, *J. Opt. Soc. Am. B* **2019**, *36*, 1108.
[13] N. E. Al-Ashi, S. A. Taya, S. A. El-Naggar, D. Vigneswaran, I. S. Amiri, *Opt Quant Electron* **2020**, *52*(3), 187-1.
[14] A. K. Pandey, M. Hashemi, *Arab J Sci Eng* **2022**, *47*, 829. https://doi.org/10.1007/s13369-021-05551-5.
[15] S. Bendib, A. Zegadi, *Arab J Sci Eng* **2017**, *42*, 2559.
[16] C. L. Wong, S. Y. Loke, H. Q. Lim, G. Balasundaram, P. Chan, B. K. Chong, E. Y. Tan, A. S. G. Lee, M. Olivo, *J. Biophotonics* **2021**, *14*(11), e202100153. https://doi.org/10.1002/jbio.202100153.
[17] K. Eom, S. Hwang, S. Yun, *J. Biophotonics* **2017**, *10*(4), 486. https://doi.org/10.1002/jbio.201600280.
[18] A. Verma, A. Prakash, R. Tripathi, *Opt. Quant Electron* **2015**, *47*, 1197.
[19] A. Panda, P. D. Pukhrambam, G. Keiser, *Appl Phys A* **2020**, *126*, 1.
[20] R. Jha, A. K. Sharma, *J. Opt. A: Pure Appl. Opt.* **2009**, *11*, 45502.
[21] Z. Lin, L. Jiang, L. Wu, J. Guo, X. Dai, Y. Xiang, D. Fan, *IEEE Photon J* **2016**, *8*(6), 1. https://doi.org/10.1109/JPHOT.2016.2631407.
[22] A. Avsar, I. J. Vera-Marun, J. Y. Tan, et al., *ACS Nano* **2015**, *9*(4), 4138.
[23] M. Bruna, S. Borini, *Appl. Phys. Lett.* **2009**, *94*(3), 3190.
[24] M. G. Daher, S. A. Taya, I. Colak, O. M. Ramahi, *Opt Quant Electron* **2022**, *54*(2), 1.
[25] S. Pal, Y. K. Prajapati, J. P. Saini, *Opt Rev* **2020**, *27*, 57.
[26] S. A. Taya, N. E. Al-Ashi, O. M. Ramahi, I. Colak, I. S. Amiri, *J. Opt. Soc. Am. B* **2021**, *38*, 2362.
[27] M. S. Rahman, M. S. Anower, M. K. Rahman, M. R. Hasan, M. B. Hossain, M. I. Haque, *Optik* **2017**, *140*, 989.
[28] M. S. Rahman, M. S. Anower, M. K. Rahman, M. R. Hasan, M. B. Hossain, M. I. Haque, *Opt Commun* **2017**, *396*, 36.
[29] A. S. Kushwaha, A. Kumar, R. Kumar, M. Srivastava, S. K. Srivastava, *Optik* **2018**, *172*, 697.
[30] M. B. Hossain, I. M. Mehedi, M. Moznuzzaman, L. F. Abdulrazak, M. A. Hossain, *Results Phys* **2019**, *15*, 102719.

How to cite this article: M. G. Daher, S. A. Taya, I. Colak, S. K. Patel, M. M. Olaimat, O. Ramahi, *J. Biophotonics* **2022**, *15*(5), e202200001. https://doi.org/10.1002/jbio.202200001